Supporting Information

Nee and Jonides 10.1073/pnas.0802081105

SI Text

SI Results. ***Brain–behavior correlations in the medial temporal lobe.*** Similar to the left mid-VLPFC, a small region in posterior parahippocampal gyrus correlated with behavioral recency (MNI center: −14, −44, −8; BA, 30; $r = 0.44$; $P = 0.059$; 7 voxels). Excluding a subject who showed parameter estimates >2.5 standard deviations from the mean strengthened this trend (MNI center: −12, −46, −10; BA, 30:19; $r = 0.56$; $P < 0.05$; 42 voxels). Like the left mid-VLPFC, this region also showed greater activation for −2 probes relative to −3 probes [$t(18) = 3.34$, $P < 0.01$], indicating that it responds to increased retrieval demands. However, visual inspection revealed that this region was difficult to disentangle from the nearby cerebellum, so we focused additional analyses on the left mid-VLPFC.

SI Discussion. ***Parietal cortex and memory.*** A recent review by Wagner and colleagues (1) synthesized a large collection of data regarding the contribution of the parietal lobes to memory. This review indicated that both the IPS and adjacent inferior parietal lobule (IPL) demonstrate strong activation increases for recognition hits relative to correct rejections. However, whereas the IPS tracked familiarity, the adjacent IPL was involved when retrieval was accompanied by additional recollective details. This fits well with the idea that the focus of attention is represented by the availability of additional semantic/conceptual information. Hence, whereas the IPS may be involved in tracking information in memory, the adjacent IPL may be involved in elaborating additional information about a given memory.

Medial temporal involvement in short-term memory. Despite short retention intervals and a low memory load, we found MTL involvement during retrieval, confirming the role of the MTL in STM. This result calls into doubt dual-store models that posit a unique role of the MTL in LTM. Instead, MTL involvement may vary with demands on retrieval, performing a similar function both for traces held online in STM and for traces that are inactive, but remnant in LTM. Recent proposals suggest that the MTL performs a domain-general relational binding function that combines item and contextual information into a coherent episodic trace (2, 3). Hence, during retrieval in both STM and LTM, the MTL may be called upon to provide contextual information during recognition decisions.

SI Methods. ***Subjects.*** Twenty-three right-handed adults (12 female, mean age = 21.4 years, range = 19–32) participated in this study with written informed consent. Four subjects were removed from imaging analyses due to motion artifacts, leaving 19 subjects for imaging analyses.

Image analysis. Whole-brain analyses were conducted using the General Linear Model implemented in SPM2. Probe-locked predictors were convolved with a canonical hemodynamic response function. Trials with incorrect responses were excluded from analysis. Contrast images for each participant were subjected to a random-effects group analysis. Whole-brain group analyses were thresholded at $P < 0.005$, uncorrected, and restricted to regions demonstrating 58 contiguous suprathreshold voxels (4). This produced a corrected cluster threshold of $P < 0.05$ (5).

To assess whether retrieval-related mechanisms differed between the most recently presented item and other information in STM, we contrasted responses to −1 probes (i.e., probes that matched the most recently presented item in each list) with those to −2 and −3 probes (i.e., probes that matched words presented in the second or first serial position in the list, respectively). To examine regions involved in short-term retrieval, we contrasted responses to −2 and −3 probes with those to −1 probes.

To investigate whether activation in IT cortex was related to behavioral performance, we examined correlations between the recency effect (faster responses in RT for −1 probes versus −2 probes), and activation (greater activation for −1 probes versus −2 probes), restricting ourselves to regions showing significant activation differences at $P < 0.01$. Notably, −3 probes were excluded from this analysis since the RT benefit (primacy effect) associated with −3 probes was presumably not associated with the focus of attention and would add unwanted noise to the analysis. The significance threshold for activation was reduced for this analysis to compensate for the reduced power, but the false-positive rate was controlled by requiring both an activation threshold as well as significant correlations with behavior. Due to signal voids near the ear canals, 4 subjects were excluded from this analysis.

To investigate whether activation in the left VLPFC and the MTL was related to behavioral performance, we examined correlations between the recency effect (faster responses in RT for −1 probes versus −2 probes), and activation (greater activation for −2 probes versus −1 probes), restricting ourselves to regions showing significant activation differences at $P < 0.01$. This analysis mirrors the analysis done on IT cortex above and once again uses a reduced activation threshold to compensate for power loss relative to our whole-brain analyses.

Follow-up functional connectivity analyses were performed using the method of Rissman *et al.* (6). To perform these analyses, we selected a seed region from right IT cortex defined as the voxels demonstrating greater activation for the −1 probe relative to the −2 and −3 probes at $P < 0.001$, uncorrected. For the left mid-VLPFC, we used the portion of cortex found to correlate with response time. These criteria produced seed clusters of 33 voxels each. Notably, several methods of seed selection could have been used and we chose to use methods that produced equal-sized seeds for both analyses.

Following the method of Rissman *et al.* (6), for each subject separate beta estimates were generated for each trial. For each different probe type, betas corresponding to that probe type were correlated with beta estimates within the seed region, producing condition-specific r-maps. R-maps were transformed into z-maps and subjected to a one-way-within-subjects ANOVA in SPM2. For the right IT analysis, contrasts examined regions demonstrating increased connectivity with the right IT seed for −1 probes relative to −2 and −3 probes. For the left VLPFC analysis, contrasts examined regions demonstrating increased connectivity with the left mid-VLPFC seed for −2 and −3 probes relative to −1 probes. Group analyses were thresholded at $P < 0.005$, uncorrected, with a 20-contiguous voxel criterion. Three subjects had to be removed from the right IT analysis due to signal voids within the region of interest.

Image acquisition and preprocessing. Images were acquired on a GE Signa 3T scanner equipped with a standard quadrature headcoil. Head movement was minimized using foam padding and a cloth restraint strapped across participants' foreheads. Experimental tasks were presented using E-Prime software (Psychology Software Tools, Inc.).

Functional T2* weighted images were acquired using a spiral sequence with 40 contiguous slices of 3.44 × 3.44 × 3 mm voxels [repetition time (TR) = 2,000 ms, echo time (TE) = 30, flip angle = 90, and field of view (FOV) = 22]. A T1-weighted

gradient-echo anatomical overlay was acquired using the same FOV and slices as the functional scans (TR = 250, TE = 5.7, and flip angle = 90). Additionally, a 106-slice high-resolution T1-weighted anatomical image was collected using spoiled gradient-recalled acquisition in steady state (specific gravity) imaging (TR = 10.5, TE = 3.4, flip angle = 25, FOV = 24, 1.5-mm slice thickness).

Each specific gravity was corrected for signal inhomogeneity (G. Glover and K. Kristoff, http://www-psych.standford.edu/~kalina/SPM99/Tools/vol_homocor.html) and skull-stripped by using FMRIb Software Library Brain Extraction Tool (http://www.fmrib.ox.ac.uk/fsl). These images were then normalized to the MNI template (avg152t1.img) using SPM2 (Wellcome Department of Cognitive Neurology, London). Functional images were corrected for slice-time differences using 4-point sinc interpolation (7) and they were corrected for head movement using MCFLIRT (8). To reduce the impact of spike artifacts, functional images were winsorized on a voxel-by-voxel basis so that no voxel had a signal greater than 3.5 SD from the mean of the run (9). Spatial normalization transformations and 8-mm FWHM isotropic Gaussian smoothing were applied to all functional images before analysis using SPM2. All analyses included a temporal high-pass filter (128 s) and each image was scaled to have a global mean intensity of 100.

1. Wagner AD, Shannon BJ, Kahn I, Buckner RL (2005) Parietal lobe contributions to episodic memory retrieval. *Trends Cogn Sci* 9:445–453.
2. Eichenbaum H, Yonelinas AR, Ranganath C (2007) The medial temporal lobe and recognition memory. *Annu Rev Neurosci* 30:123–152.
3. Davachi L (2006) Item, context, and relational episodic encoding in humans. *Curr Opin Neurobio* 16:693–700.
4. Forman SD, *et al.* (1995) Improved assessment of significant activation in functional magnetic resonance imaging (fMRI): Use of a cluster-size threshold. *Magn Reson Med* 33:636–647.
5. Slotnick SD, Moo LR, Segal JB, Hart J (2003) Distinct prefrontal activity associated with item memory and source memory for visual shapes. *Cogn Brain Res* 17:75–82.
6. Rissman J, Gazzaley A, D'Esposito M (2004) Measuring functional connectivity during distinct stages of a cognitive task. *NeuroImage* 23:752–763.
7. Oppenheim AV, Schafer RW, Buck JR (1999) *Discrete-Time Signal Processing* (Prentice Hall, Upper Saddle River, NJ), 2nd Ed.
8. Jenkinson M, Bannister P, Brady M, Smith S (2002) Improved optimization for the robust and accurate linear registration and motion correction of brain images. *NeuroImage* 17:825–841.
9. Lazar NA, Eddy WF, Genovese CR, Welling J (2001) Statistical issues in fMRI for brain imaging. *Int Stat Rev* 69:105–127.

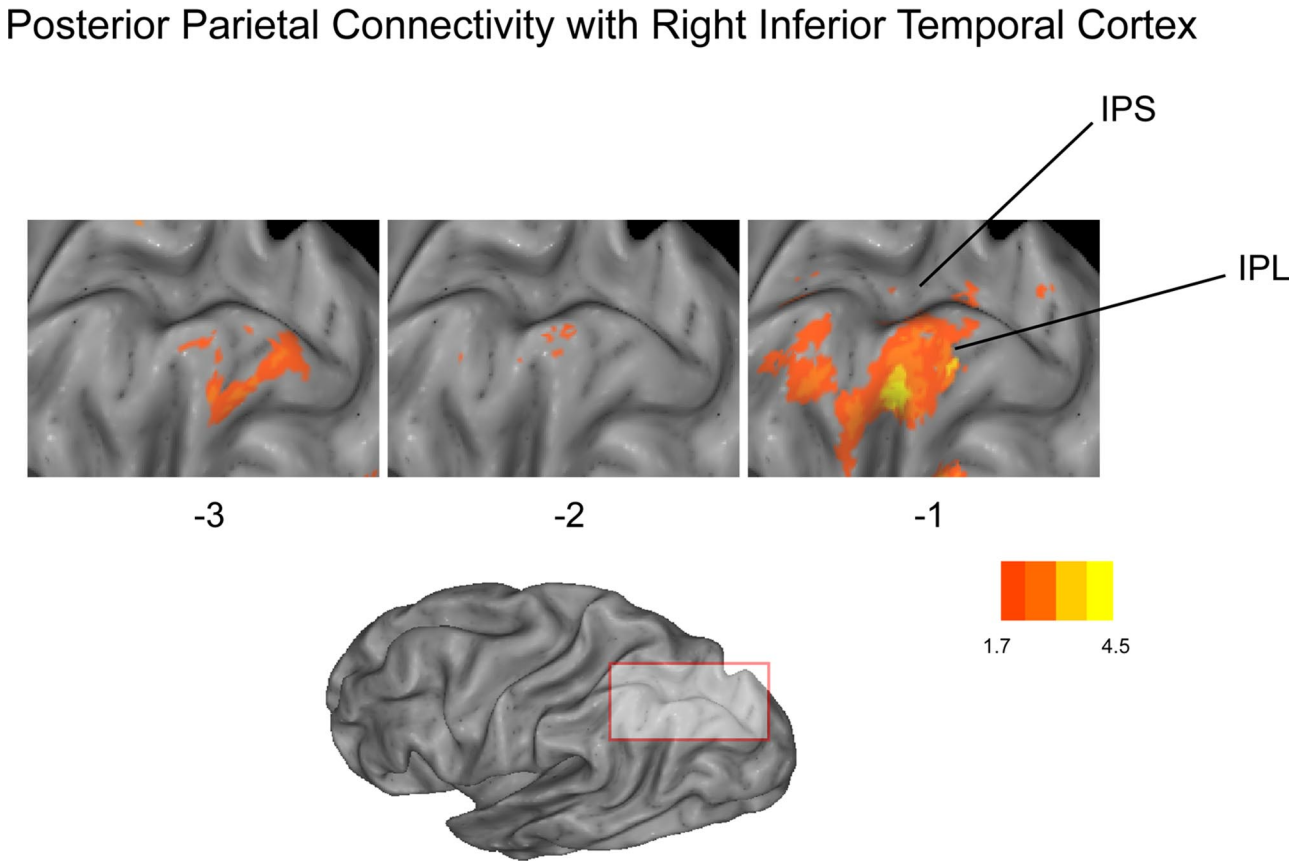

Fig. S1. Functional connectivity with right IT for −3 probes, −2 probes, and −1 probes. The focus of attention (−1 probes) was associated with enhanced functional connectivity in the IPL adjacent to the intraparietal sulcus. Results thresholded at $P < 0.05$ [t (30) = 1.7] for display purposes.

Table S1. Behavioral data

Probe type	Neg	−3	−2	−1
Accuracy (%)	96.0 (5.0)	94.5 (6.5)	92.7 (8.4)	94.5 (6.3)
RT (ms)	549.3 (67.6)	541.0 (71.4)	563.0 (75.6)	515.9 (62.3)

Summary of the behavioral data. SD are in parentheses. RT, reaction time.

Table S2. Neural correlates of the focus of attention

Region	X	Y	Z	Voxels	T-value	BA
Right inferior temporal gyrus	62	−22	−20	123	4.74	21/20
	62	−30	−16		3.98	
Left inferior temporal gyrus	−52	−18	−24	81	4.18	20/21
	−60	−22	−24		3.64	

Contrast of −1 probes versus −2 and −3 probes. Whole-brain results reported at $P < 0.005$ with 58 contiguous voxels or more, producing a corrected cluster threshold of $P < 0.05$. X, Y, and Z denote peaks in MNI space. BA, Brodmann areas.

Table S3. Neural correlates of short-term retrieval

Region	X	Y	Z	Voxels	T-value	BA
Frontal						
Left dorsolateral PFC	−54	20	30	185	4.96	9/46
Left mid-ventrolateral PFC	−56	30	22		4.21	45
Temporal						
Left parahippocampal/entorhinal cortex	−24	−34	−20	277	4.66	36/35
	−12	−46	−8		4.3	30/19
Left superior temporal gyrus	−62	−54	12	80	4.5	22
Left posterior insula	−40	−16	−6	71	4	13
Left superior temporal sulcus	−54	−2	−8	93	3.76	21/22
	−68	−4	−6		3.7	
	−62	2	−14		3.29	

Contrast of −2 and −3 probes versus −1 probes. Whole-brain results reported at $P < 0.005$ with 58 contiguous voxels or more, producing a corrected cluster threshold of $P < 0.05$. X, Y, and Z denote peaks in MNI space. BA, Brodmann areas; PFC, prefrontal cortex.

Table S4. Functional connectivity interactions with the focus of attention

Region	X	Y	Z	Voxels	T-value	BA
Frontal						
Right ventrolateral PFC (including anterior insula and superior temporal gyrus)	46	18	−14	142	4.55	47/38
Right premotor	24	0	70	26	3.65	6
Ventral medial PFC	4	44	−14	157	3.52	11
	4	46	−12		3.25	
	−4	46	−12		2.99	
Dorsal medial PFC	2	42	32	202	3.43	9
	−4	44	22		3.21	
	4	48	26		3.19	
Right anterior medial PFC	4	54	8	42	3.26	10
Temporal						
Left superior temporal gyrus	−50	16	−10	29	3.47	38
Left inferior temporal gyrus	−68	−14	−16	28	3.25	21
Parietal/occipital						
Left inferior parietal lobule	−42	−68	34	33	3.54	39
Left precuneus/PCG	−18	−74	28	20	3.12	31/7
Left retrosplenial cortex/PCG	−8	−42	16	345	4.65	29/30
Left lingual gyrus	−14	−66	−8		3.54	19/18
	−10	−58	−6		3.26	
Right lingual gyrus	10	−66	−2	28	3.16	18/19
Right calcarine sulcus	4	−78	0	202	4.18	18
	12	−86	0		2.79	
Other						
Left putamen	−12	8	−18	100	4.01	
	−24	6	−12		3.05	
Right putamen	18	18	−12	20	3.25	
Midbrain/thalamus	−6	−12	−6	148	3.76	
Thalamus	2	−24	14	50	3.29	
	4	−14	12		3.26	

Function connectivity with right inferior temporal cortex. Contrast of connectivity for −1 probes versus −2 and −3 probes. Whole-brain results reported at $P < 0.005$ with 20 contiguous voxels or more. X, Y, and Z denote peaks in MNI space. BA, Brodmann areas; PFC, prefrontal cortex; PCG, posterior cingulate gyrus.

Table S5. Functional connectivity interactions with retrieval-demands

Region	X	Y	Z	Voxels	T-value	BA
Frontal						
Left anterior ventrolateral PFC	−44	36	−12	31	3.11	47/11
Ventromedial PFC	6	46	−24	54	4.1	11
Temporal						
Left hippocampus	−24	−14	−14	41	3.43	
Left hippocampus	−34	−30	−10	40	3.32	
Left anterior STG	−58	2	−10	102	4.67	21/38
	−50	6	−12		3.38	
Left posterior STG	−70	−36	6	56	3.43	22/42
	−68	−50	−2		3.08	
Left STG/inferior parietal lobule	−70	−26	12	33	3.77	42/40
Right STG/inferior parietal lobule	−70	−24	14	23	3.33	42/40
Occipital						
Left cuneus/precuneus	−22	−82	20	41	3.74	18/31
Left lingual gyrus	−2	−90	−12	20	3.23	18
Left middle occipital gyrus	−28	−92	12	20	3.11	19

Functional connectivity with left mid-ventrolateral prefrontal cortex. Contrast of connectivity for −2 and −3 probes versus −1 probes. Whole-brain results reported at $P < 0.005$ with 20 contiguous voxels or more. X, Y, and Z denote peaks in MNI space. BA, Brodmann areas; PFC, prefrontal cortex; STG, superior temporal gyrus.